

Raman spectroscopic analysis of carbonaceous material in Longmenshan fault zone at Shenxigou

KOUKETSU, Yui^{1*} ; SHIMIZU, Ichiko¹ ; YAO, Lu² ; MA, Shengli² ; SHIMAMOTO, Toshihiko²

¹Graduate School of Science, The University of Tokyo, ²State Key Laboratory of Earthquake Dynamics Institute of Geology, China Earthquake Administration

On 12th May 2008, Wenchuan M_W 7.9 earthquake occurred along the Longmenshan thrust belt between the Tibetan plateau and the Sichuan basin. Shenxigou area is located at the western end of the coseismic faults during the Wenchuan earthquake. The fault zone consists of fault gouge, fine fault breccia, and fault breccia. The gouge zone consists of grayish gouge (GG) and blackish gouge (BG). The breccia zone consists of grayish breccia (GB), blackish breccia (BB), and mixtures (Mix) of GB and BB. The concentrations of organic carbon are reported as less than 1 wt.% in GG and GB, while those in BG and BB are 28 and 36 wt.%, respectively (Wang et al. 2014; Earthquake Science) . In the present study, we performed the Raman spectroscopic analysis of carbonaceous material (CM) included in these fault rocks and host sedimentary rocks. In addition to the natural samples, we also analyzed the gouge samples after high-velocity frictional experiment to detect the structural change of CM by frictional heating.

Raman spectroscopic analysis was carried out using 532 nm Nd-YAG laser. The laser power was limited to 0.2 mW to avoid the damage to CM. The CM Raman spectrum was fitted using four peaks (D1, D2, D3, and D4 bands) following the method of Kouketsu et al. (2014; Island Arc). The Raman spectra of CM in GG, BG, GB, BB, and Mix were similar, and all Raman spectra indicated that the structure of CM corresponds to amorphous carbon. This result suggests that the carbons were originated from the organic materials in the host rocks and not concentrated by hydrothermal precipitation. The Raman band width (full width at half maximum; FWHM) of these fault rocks was larger than that of the host rock, and it means that the degree of coalification of CM in the fault rock is lower than the host rock. The estimated metamorphic temperatures using Raman CM geothermometer proposed by Kouketsu et al. (2014) are around 200-230 °C in the fault rocks and 280-300 °C in the host rock. The Raman spectra of CM in the sample conducted on the frictional experiment that was carried out at constant slip rate of 1.4 m/s and normal stresses 0.8 MPa under room humidity conditions using BG also showed no obvious change compare to those of CM before the experiment. In the present study, frictional heating was not detected by the Raman spectroscopy in natural and experimental fault samples. These results indicate that the heating duration of the coseismic slip was insufficient for the studied CM to mature enough.

Keywords: Wenchuan earthquake, Longmenshan fault system, Carbonaceous material, Raman spectroscopy, Frictional heating

Detection of past frictional heating on fault from Raman spectra of carbonaceous material

TABATA, Hiroki^{1*} ; UJIIE, Kohtaro¹ ; KOUKETSU, Yui² ; KAGI, Hiroyuki²

¹University of Tsukuba, ²Graduate School of Science, The University of Tokyo

Raman spectra of carbonaceous material (RSCM) systematically change with increases in temperature and thus have been used as a geothermometer in sedimentary and metamorphic rocks. We examined whether RSCM can be useful to detect increased temperatures associated with frictional heating on fault. The studied fault constitutes the thrust sheet boundary in the coherent chert-clastic sequence of the Jurassic accretionary complex in central Japan. The fault includes a few millimeters-thick, chert-derived pseudotachylyte and the 50-cm-thick cataclasite defined by the fragments of black chert in the carbonaceous clay matrix. We analyzed RSCM with a 514.5 nm Ar⁺ laser across these fault rocks and obtained characteristic Raman bands. The results show that the intensity ratio of D1-band and D2-band (I_{D1}/I_{D2}) and the full width at half maximum (FWHM) of the D1-band markedly decrease in the pseudotachylyte and the host rocks (gray chert) of less than ~2 mm from upper and lower boundaries of the pseudotachylyte, representing the localized progress in carbonization. In contrast, there are no changes in I_{D1}/I_{D2} and FWHM of the D1-band across the boundaries of the cataclasite. The spatial distribution of the decreased I_{D1}/I_{D2} and FWHM of the D1-band and the presence of pseudotachylyte are consistent with the localized heating during frictional melting along a few millimeters-thick slip zone. We conclude that RSCM is useful to detect increased heating associated with seismic slip on faults.

Keywords: carbonaceous material, Raman spectra, pseudotachylyte, cataclasite, chert-clastic sequence

Effect of humidity on frictional healing of montmorillonite

TETSUKA, Hiroshi^{1*} ; KATAYAMA, Ikuo¹

¹Department of Earth and Planetary Systems Science, Hiroshima University

According to time-predictable model for characteristic earthquakes, a stress increases at a constant ratio in interseismic period, and an earthquake occurs when the stress reaches a certain constant stress (Shimazaki and Nakata, 1980). This model has been applied for long-term forecasts for the Tokai earthquake, the Nankai earthquake. The ratio of stress increasing depends on the frictional healing effect which is the effect of the strength recovery with logarithm of hold time. In subduction-zones, smectite plays a key role for frictional behavior in surfaces of oceanic plates, and which has shown very low coefficient of friction (Ikari et al., 2007; Ujiie et al., 2013). Moreover, water distribution, hence humidity, contribute to the non-uniform clay minerals and its saturation along subduction-zones (Zhao et al., 2009). Previous studies investigated the effect of humidity on frictional healing of bare quartzite and quartz, alumina and soda-lime glass powders, which results that the frictional healing increases with increasing relative humidity (Dieterich and Conrad, 1984; Frye and Marone, 2002; Scuderi et al., 2014). However, the effect of humidity on the frictional healing of smectite has not well understood, therefore, we examined the effect of humidity on frictional healing of montmorillonite (a type of smectite) with comparison to quartz.

We conducted slide-hold-slide test (10, 30, 100, 300, 1000, 3000s) at 15MPa normal stress and $3\mu\text{m/s}$ shearing velocity. The experiment are carried out at four humidity conditions, 1) in deionized water with a water tank at room temperature, 2) at room temperature and humidity, 3) at room temperature and humidity after having been dried samples at 100 °C for 24 hours, 4) at 100 °C with a heater after having been dried samples at 100 °C for 24 hours.

We found the result that the frictional healing of montmorillonite decreases with increasing relative humidity, which is opposite to that observed in the experiments for quartz. The negative correlation between frictional healing effect and relative humidity on montmorillonite can be explained by the weakness of interlamellar cohesion due to expanding distance between layers in montmorillonite.

The smaller the frictional healing effect, the smaller stress recover in interseismic period. Assuming that the time-predictable model is correct, the smaller stress recover in interseismic, the longer recurrence time of earthquakes. Therefore, it is expected that the recurrence time of earthquakes is long in areas are wet and in which montmorillonite abound.

Keywords: smectite, frictional healing, humidity

Sample preparation condition for SEM-EBSD: An example of quartz minerals in granite

KANAI, Takuto^{1*}; MUKOYOSHI, Hideki²; TAKAGI, Hideo³

¹Graduate school of creative science and engineering, Waseda University, ²Interdisciplinary Graduate School of Science and Engineering, Shimane University, ³Faculty of Education and Integrated Arts and Sciences, Waseda University

Electron Backscatter Diffraction (EBSD) is used to determine a crystallographic orientation of the mineral in the Scanning Electron Microscope (SEM). For rock samples, thin section is generally used for EBSD analysis. Mechanical polishing of thin sections with diamond paste cause damages to the lattices of minerals at the specimen surface. Thus, additional processes of vibratory chemical-mechanical polishing with colloidal silica suspension is required to remove the mechanical damage (e.g., Prior et al., 1999; Lloyd, 1987). Although a number of study of EBSD for rocks are published, there is little report of detailed procedure or optimum conditions for thin section preparation with colloidal silica vibratory polishing. The objective of this study is to examine the optimum conditions of rock sample preparation, especially time and normal load of vibratory polishing, for EBSD analysis using quartz crystals in granite.

Vibratory polishing were conducted using VibroMetTM 2 vibratory polisher (BUEHLER Inc.) with colloidal silica suspension (Model No.: 5904-S-64, pH: 9.8, particle size: 40 nm) (PRECISION SURFACES INTERNATIONAL Inc.).

Examined conditions of vibratory polishing with colloidal silica suspension were as follows:

Time: 0, 60, 120, 180 minutes

Normal load: weight (200 g)×1, weight (200 g)×3

The EBSD analyses were performed at the Waseda University with an automated electron back-scattered diffraction system (Channel5, HKL) attached to a SEM (HITACHI S-3400N) with a tungsten filament, an accelerating voltage of 25 kV, a working distance of 30 mm, and with the specimens tilted 70°. Coating the specimen with a conductive material such as carbon removes the problem of charge build-up, but reduces the quality of Electron Backscattering Patterns (EBSPs). To eliminate the problem, EBSD analyses were performed under low-vacuum condition (30Pa) without coating. We selected 20 quartz grains per samples under the BSE image and 70×70 μm area with 2 μm step size (total 1225 points) were measured for each grains. To evaluate the effects of the different vibratory polishing steps on EBSD pattern quality, hit rate which is percentage of value of correctly indexed points to total measured points was used.

The results of 0 minute vibratory polished sample (only diamond polishing) shows less than 55% of hit rate. After 60 minutes of colloidal silica polishing, 70% of the points are correctly indexed, while after 180 minutes this value increases to around 80%. Significant difference of effect of weight was not found. This result shows 60 minutes vibratory polishing is enough for EBSD analysis of quartz grain in granite. For another minerals or rock type, further examination might be required.

Keywords: SEM-EBSD, colloidal silica, vibratory polishing, thin section

Fault Lubrication and Billow-like Wavy Folds in a Seismic Slip Plane of Nojima Fault Gouge: Rock Magnetic Perspective

FUKUZAWA, Tomohiko^{1*} ; NAKAMURA, Norihiro¹

¹Graduate School of Science, Tohoku University

An earthquake can occur only if friction decreases rapidly as slip proceeds and the shear stress on its fault planes surpasses the frictional strength of faults, indicating frictional coefficients significantly decrease (0.7→0.1) in proportion to a displacement. High-velocity friction experiments have proposed thermal pressurization and fluidization as weakening mechanism of a frictional strength of faults, but few geological traces for this mechanism are left behind in a natural fault zone. Asymmetric folding and fluttering structures have been found in a natural fault zone, such as in Nojima active fault and in Kodiak accretionary prism. In Nojima fault gouge, it is well known that there are billow-like wavy folds along slip planes, being similar to the pattern of Kelvin Helmholtz (KH)-instability which normally occurs in fluid. This instability generates at the interface between two fluids of different densities shearing at different velocities (Thorpe, 2005). Therefore, the presence of billow-like wavy folds in Nojima fault gouge suggests the fluidization of gouge materials. If a temperature range for the generation of such billow-like folds could be determined, one can give a constraint to the weakening mechanism of frictional strength of faults. Here I show rock magnetic studies to prove the temperature rise in the generation of billow-like folds in cohesive blackish gouges, using a custom-made scanning magneto-impedance magnetic microscope. The results showed the billow-like folds and the sharp slip zones experienced at least a 375 °C heating during its formation from the incohesive grayish gouges, because of the magnetite formation through thermal decomposition of siderite in the grayish gouge. The upper limit of temperature rises can be constrained as at maximum 800 °C by the preservation of microfold textures because high viscosity fluid, such as melt, can't generate a shear flow forming KH-instability. Based on these results, these two zones had been experienced a frictional heating (375 °C ~800 °C). From the temperature condition and the one-dimensional diffusion model, I estimated the frictional coefficient of a fault zone in Nojima fault gouge is approached to be 0.02~0.04 during coseismic slip. These results indicate that thermal pressurization-induced fluidization occurred in the fault slip.

The fragmentation and alteration history of fault rocks in the Byobuyama fault, Gifu Prefecture, central Japan.

KATORI, Takuma^{1*} ; KOBAYASHI, Kenta¹ ; YASUE, Ken-ichi² ; NIWA, Masakazu² ; KOMATSU, Tetsuya² ; HOSOYA, Takushi³ ; SASAO, Eiji²

¹Department of Geology, Faculty of Science, Niigata University, ²Japan Atomic Energy Agency, ³Chuo Kaihatsu Corporation

The Chubu region is one of the most concentrated area of active faults. These are roughly classified into two orthogonally-oriented fault sets of NE-SW and NW-SE strikes. The Byobuyama fault, 32 km in length, is NE-SW strike and located in the boundary of the Mikawa and Mino plateaus. It displaces perpendicularly the Pliocene Toki Sand and Gravel Formation by 500 m. This fault's northeastern edge has contact with the southern edge of the Atera fault of NW-SE strike and offset their displacements each other. It is clear that the activity of the Byobuyama fault has affected topographical development in this area and also plays a role of the development of the complicated fault geometry system in the Chubu region. In this study, we performed structural and chemical analyses of fault rocks of the Byobuyama fault, as a case study for improving research technique to reveal the history of active faults.

Studied outcrop is located in Rontochi area in Mizunami city, Gifu Prefecture. This is a newly discovered outcrop of the Byobuyama fault. Wide brittle fracture zone along the boundary of the Toki Sand and Gravel Formation and Inagawa Granite is identified in this outcrop. Strike and dip of the fault plane is N42E50SE. This outcrop can include the master fault of the Byobuyama fault based on the fault trend, scale of the fracture zone, the relationship dividing the Toki Sand and Gravel Formation and Inagawa Granite, and with the location along the active fault trace. The fracture zone consists of light brown fault breccia (>30 cm thick) derived from the Toki Sand and Gravel Formation, brown fault gouge (about 30 cm thick) derived from the Toki Sand and Gravel Formation, reddish brown fault gouge (about 5 cm thick) derived from the Toki Sand and Gravel Formation, white foliated cataclasite (about 40 cm thick) derived from the granite, white cataclasite (about 30 cm thick) derived from the granite, and weak crushed granite in order from footwall to hanging wall. Deep green fault gouge injects into the foliated cataclasite. At this outcrop, we collected samples for structural and chemical analyses. Samples of non-cohesive fault rocks are fragile because of abundant swellable clay minerals. We referred to Takagi & Kobayashi (1996) and Oohashi et al. (2008) for suitable sample collection, solidification, cutting and polishing. As a chemical analysis, we performed XRD and XRF analyses.

Based on these structural and chemical analyses, the Byobuyama fault has experienced activities of several stages under different stress field. The fault rocks contain smectite, illite and kaolinite as a whole. Especially, the fault rocks derived from the granite also contain zeolite. In addition, we can see a trend that increasing Mg, Ca and LOI, and decreasing Na of the fault rocks. Degree of variability of elements is highest in the fault core.

In this presentation, we discuss the fragmentation and alteration history of fault rocks through the development of the Byobuyama fault.

This study was carried out under a contract with METI (Ministry of Economy, Trade and Industry) as part of its R&D supporting program for developing geological disposal technology.

Keywords: Byobuyama fault, fault rocks, fragmentation, alteration, clay mineral

Permeability evolution of oceanic basalt at Nankai subduction zone: implication from on shore basalt at Shimanto belt

TANIKAWA, Wataru^{1*} ; YAMAGUCHI, Asuka² ; HAMADA, Yohei¹ ; KAMEDA, Jun³ ; TADAI, Osamu⁴ ; HATAKEDA, Kentaro⁴

¹JAMSTEC/KCC, ²Tokyo University, ³Hokkaido Univeristy, ⁴Marine Works Japan. LTD

A large slip displacement was observed at shallow portion of the plate boundary fault during 2011 Tohoku earthquake, and this slip has contributed to cause a huge tsunami disaster. One of possible mechanisms that caused the large slip is a formation of excess pore pressure zone, which can reduce the fault strength for a long period of time, at middle to deeper portion of subduction zone. The excess pore pressure can be generated by chemical dehydration, fluid influx from deeper crust and pore volume reduction which associates with permeability reduction at a large subduction plate boundary. The same process would be caused at the Nankai Subduction zone as well. Fluid transport properties (i.e. permeability, porosity) and their changes during subduction can strongly influence on the pore pressure generation. In the present study, the evolution of fluid transport properties for oceanic basalt at Nankai Subduction zone are investigated by measuring the transport properties for basaltic rocks from the on shore Shimanto belt, South-western Japan.

We collected basalt brocks in the Cretaceous Shimanto accretionary complex of Japan from Okitsu-Kozurutsu, Kure, Mugi (Upper and Lower), and Makimine sites in the southeast Japan. Vitrinite reflectance value, R_o , that is the indicator of the maximum experienced temperature, ranges from 1 to 4.5 in our samples. The basalt from Lower Mugi site shows the lowest value, and the largest value is observed in Makimine site. We measured porosity, elastic wave velocity, and rock electric resistivity of each basalt at atmospheric pressure and room temperature. Permeability was measured at room temperature and under confining pressure from 1 to 160 MPa. The steady state gas flow method was applied to evaluate the permeability by using N_2 gas as a pore fluid. Pore pressure at the upper end of the specimen was kept at constant pressure from 0.05 to 2 MPa to apply constant differential pressure, and mass flow rate at atmospheric pressure that flows out from the lower end of the specimen was measured.

The permeability testing results show gas permeability was proportional to the inverse of the pore pressure at the same confining pressure. This trend agrees with the Klinkenberg effect, therefore most of the gas permeability data were transformed to 'water' permeability using the relationship between gas permeability and pore pressure. Permeability of all samples decreased with an increase of confining pressure, and permeability decreased three orders of magnitude by increasing confining pressure from 5 to 120 MPa. Permeability was lower for more matured basalt, and permeability of the Lower Mugi basalt was $7 \times 10^{-18} \sim 9 \times 10^{-19} \text{ m}^2$ and that of Makimine basalt showed the lowest value of $2 \times 10^{-22} \text{ m}^2$. Variation of permeability in the same unit varied from 1 to 2 orders of magnitude. Pore diameters for all samples showed less than $0.01 \mu\text{m}$, which is the lower limit of the machine.

Permeability reduction by the diagenesis is consistent with the reduction of porosity, and this indicates that a reduction of pore diameter and pore volume induced by a mechanical and chemical compaction during subduction caused gradual permeability reduction. Internal structure of basalt observed from the μX -ray CT image suggests the variation of the permeability in the same unit is influenced by the variation of fracture density for the basalts.

Our results suggest that both pore volume and permeability reductions can significantly contribute to pore pressure generation. Therefore, timing and area of high pore pressure generation can be controlled by the evolution of permeability and porosity with subduction.

Keywords: permeability, diagenesis, pore pressure, Nankai earthquake, Shimanto belt, basalt

Lithology and fluid transport property of the topmost part of the oceanic crust subducting into the Nankai Trough

YAMAGUCHI, Asuka^{1*} ; TANIKAWA, Wataru² ; TADAI, Osamu³ ; KAMEDA, Jun⁴

¹Atmosphere and Ocean Research Institute, the University of Tokyo, ²Japan Agency for Marine-Earth Science and Technology, Kochi Institute for Core Sample Research, ³Marine Works Japan, ⁴Earth and Planetary System Science Department of Natural History Sciences, Graduate School of Scienc

Fluids in subduction plate boundaries play important roles for both mechanical and chemical aspects. Recently, oceanic crust has been recognized as a source of water along seismogenic subduction plate boundary (Kameda et al., 2011). For documenting hydration state of topmost part of subducting oceanic crust, we performed visual, optical and Electron Probe Micro Analyzer (EPMA) observations and powder X-ray Diffraction (XRD) analyses of basaltic rocks retrieved from the Site C0012 of Integrated Ocean Drilling Program (IODP) Expedition 333. We also measured porosity and permeability of samples selected from each lithology. We further interpreted Logging-while-drilling (LWD) data of Hole C0012H obtained during the IODP Expedition 338 to estimate the thickness of seafloor alteration.

The IODP Site C0012 is located at the top of Kashinozaki Knoll, tectonically uplifted topographic high on the Philippine Sea Plate coming into the Nankai Trough. Basaltic rocks in Holes C0012A, E, F, G occurring below 520 mbsf, are mainly composed of upper pillow basalts and lower massive basalts. The pattern of alteration is lithology-dependent: in pillow basalts, volcanic glasses and vesicles were replaced by clay minerals; while alteration of massive basalt showing doleritic texture is characterized by red-colored Fe-oxyhydroxide veins with alteration halos. Potassium-bearing alteration minerals (K-feldspar and celadonite) occur in places.

Permeability measurement of representative samples of each lithology was performed at JAMSTEC-Kochi, under the room temperature conditions with effective pressures of 5 to 120 MPa. Permeability was measured by using N₂ gas as a pore fluid, and calculated by steady-state gas flow method. Gas permeability decreases with increasing effective pressures and pore pressures, following the Klinkenberg equation. Klinkenberg-corrected permeability of pillow basalt ranges 10-19 to 10-20 m² at effective pressure of 5 MPa, while that of massive basalt ranges 10-17 to 10-19 m². Permeability contrast between the two lithologies would reflect microtextural difference between two lithologies, because of the absence of significant difference in porosity.

LWD data of basaltic rocks were obtained from Hole C0012H of the IODP Expedition 338. Low resistivity and velocity intervals are corresponding to pillow basalts, whereas high resistivity and velocity intervals are corresponding to massive basalts. Contrastingly, gamma ray trend is independent from resistivity and velocity trends: positive at around lithological boundaries. Positive peaks of gamma ray would reflect potassium-bearing alteration caused by permeability contrast between each lithology. Below 680 mbsf, all logging data become constant and non-fluctuated, suggesting that lithology become homogeneous below this depth without strong alteration. Therefore the thickness of hydrated part of oceanic crust at Site C0012 is roughly estimated to be ~100 m.

Laboratory experiments on dynamic rupture propagation using rocks

MIZOGUCHI, Kazuo^{1*}

¹Central Research Institute of Electric Power Industry

Around pre-existing geological faults in the crust, we have often observed off-fault damage zone where there are many fractures with various scales, from $\sim\mu\text{m}$ to $\sim\text{m}$ and their density typically increases with proximity to the fault. One of the fracture formation processes is considered to be dynamic shear rupture propagation on the faults, which leads to the occurrence of earthquakes. Although much work on such off-fault damage associated with dynamic rupture in homogeneous material (ex. polymers) have been done in the past decades (Rosakis et al., 2007), the rupture-induced damaging behavior of rocks, that constitute the faults in nature and of which frictional properties controlling the dynamic rupture might be different from the polymers, is still experimentally unexamined.

Recently, I have worked on laboratory experiments on dynamic rupture propagation along contacting surfaces of two metagabbro blocks from Tamil Nadu, India, simulating a fault of 30 cm in length. For the experiments, the similar uniaxial loading configuration to Rosakis et al. (2007) is used. Axial load σ is applied to the fault plane with an angle θ to the loading direction. Changing the angle makes the ratio of shear to normal stress on the fault a critical level close to the maximum static frictional strength beyond which the fault begins to slip spontaneously. For the critically stressed fault, the triggering of rupture is archived by striking the one edge of the fault with a hammer and the subsequent increase in shear load for a short duration. The load cell attached to the tip of the hammer head can provide us the magnitude and time duration of the impact stress. In this presentation, I introduce the experimental set-up and some preliminary results for the dynamic rupture propagation on rocks. This work is supported by the JSPS KAKENHI (26870912).

Keywords: Dynamic rupture propagation, Rock, Fault, Experiment

Temperature-dependent frictional strength of dolerite in a nitrogen atmosphere

TANAKA, Nobuaki^{1*} ; WADA, Jun-ichi² ; KANAGAWA, Kyuichi¹

¹Graduate School of Science, Chiba University, ²OYO Corporation

Since mid-1990's, high-speed (up to several m/s; equal to coseismic slip rate) friction experiments on variable rocks have revealed that frictional strength significantly decreases with increasing slip rate ≥ 10 cm/s. However, frictional strength possibly decreases due to increased temperatures because the past high-speed friction experiments have not controlled temperatures increased by frictional heating. In fact, friction experiments on dolerite at a normal stress of 1 MPa, a slip rate of 1 cm/s, controlled temperatures up to 1000 °C and in air showed that the decrease in frictional strength at fast slip rates is possibly due to increased temperatures (Noda et al., 2011, JGR). These experiments also showed that the temperature-dependent frictional strength of dolerite has a negative correlation with the amount of amorphous wear material as well as a positive correlation with the amount of iron oxides formed by oxidation of iron-bearing minerals. However, oxidation of iron-bearing minerals as observed in the experiments is unrealistic in fault zones at depths due to the paucity of oxygen there.

We therefore have conducted similar friction experiments on dolerite as Noda et al. (2011) in a nitrogen atmosphere with an oxygen concentration of 0.1 %, and investigated the dependence of steady-state frictional strength on temperature and its relation to the amount of amorphous wear material and the ratio of wear material cover on the slip surface. The steady-state friction coefficient was ~ 0.52 at room temperature, while it was ~ 0.7 being roughly constant at 100-500 °C and ~ 0.76 at 600 °C. The amount of amorphous material ranged within 60 ± 6 wt% from room temperature to 500 °C and ~ 38 wt% at 600 °C. The ratio of wear material cover on the slip surface was ~ 0.78 at room temperature, while it was ~ 0.9 being roughly constant at 100-600 °C. The steady-state friction coefficient of dolerite in a nitrogen atmosphere is significantly lower than that in air (~ 0.77) at room temperature, while it is larger than the latter (0.61 ± 0.03) at temperatures from 100-600 °C. It shows a negative correlation with the amount of amorphous material as observed in air at 100-600 °C, while it also shows a positive correlation with the ratio of wear material cover at room temperature to 500 °C. However, the former and latter correlations become unclear at room temperature to 100 °C and at 500-600 °C, respectively.

The frictional strength of dolerite at room temperature significantly lower in a nitrogen atmosphere than in air is likely due to the lack of moisture-adsorbed strengthening. However, the reason for higher frictional strength in a nitrogen atmosphere than in air at 100-600 °C is unknown at present. It is also unknown at present what are responsible for the correlations among temperature-dependent frictional strength, the amount of amorphous material and the ratio of wear material cover. These are the subjects of our future study.

Keywords: Dolerite, Nitrogen atmosphere, Rotary shear experiment, Temperature dependency, Amount of amorphous wear material, Ratio of wear material cover

Relation between mainshock rupture and aftershock sequence based on highly resolved hypocenters and focal mechanisms

YUKUTAKE, Yohei^{1*} ; IIO, Yoshihisa²

¹Hot Springs Research Institute of Kanagawa Prefecture, ²Disaster Prevention Research Institute, Kyoto University

To understand a generation process of aftershock following a large earthquake, it is essentially important to elucidate whether an aftershock reflects re-rupture of mainshock fault plane or rupture of damage zone surrounding it. Liu et al. (2003) found that only a small portion of the aftershocks occurred on the rupture fault planes of the 1992 Landers Earthquake. However, since the location errors of the aftershock hypocenters in their study were up to 1 km, discussion based on more precisely determined hypocenters is essential.

A dense seismic observation network composed of 59 temporary stations was installed, immediately after the 2000 Tottori-Ken Seibu Earthquake (Mw 6.8). The high quality observation data gives us an excellent opportunity to clarify the above issue. To obtain highly resolved hypocenter locations, we used the Double Difference relocation method (Waldhauser and Ellsworth, 2000). Then, we used the differential travel time data determined from manually picked arrival times and cross-correlation analysis. We could determine the hypocenters of approximately 4,100 events that occurred during the period from October, 15 and November, 31, 2000. We also could obtain the focal mechanisms of 3,300 events, by using absolute amplitude data of P and SH waves, as well as P wave polarities.

Since surface faulting were not immersed above the aftershock region of the Tottori-Ken Seibu Earthquake (Ueta et al., 2002), we estimated subsurface structure of the mainshock fault planes on the basis of the relocated hypocenter and focal mechanisms distributions. Since we could see several 'earthquake clusters' that possess similar characteristic of focal mechanism, we divided the aftershock distribution (except the northern part of the aftershock region) into 5 earthquake clusters. We estimated the best-fit plane in each earthquake cluster, by using principal component analysis (e.g. Shearer et al., 2003).

We could obtain 5 best-fit planes. Trends of the best-fit planes near the mainshock hypocenter and southern part of the aftershock region are consistent with those of mainshock focal mechanism obtained from P wave polarities and CMT analysis, respectively. On the other hand, in the northern part of the mainshock hypocenter, the best-fit planes suggesting conjugate fault were estimated. We found that most of the aftershocks in each earthquake cluster were distributed within zones of approximately 1.2 km width, rather than aligned on a single plane. We also evaluated the variety of focal mechanisms by using the Kagan angle (Kagan, 1991) from reference focal mechanisms that were estimated based on the best-fit planes. We found that the focal mechanisms of the aftershocks have wide range of the Kagan angle ($\leq 100^\circ$). These results suggest that many aftershocks represent rupture within fault damage zone around the mainshock rupture planes. The wide variations of focal mechanisms probably reflect the complicate structure in the fault damage zone.

Keywords: Aftershock, Hypocenter distribution, Focal mechanism, Mainshock fault

Earthquake sequence simulations using measured frictional properties for JFAST core sample

NODA, Hiroyuki^{1*} ; SAWAI, Michio² ; SHIBAZAKI, Bunichiro³

¹JAMSTEC, ²Hiroshima University, ³Building Research Institute

Parameters in a rate- and state-dependent friction law (RSF) are often determined by velocity-step tests in which the slip rate V is stepped typically by a factor of 3 to 10. The test may yield a set of parameter values such as a , b , and d_c , but it is often the case that those determined parameters depend on V if a logarithmically wide range of V is investigated. At this point, the originally assumed constitutive law is shown to be invalid, strictly speaking, and thus need to be modified. For example, the experiments by Dieterich [1978] show that the rate-dependency $\partial f_{ss}/\partial \ln(V)$ increases as V increases, which can be explained by introduction of a cut-off time for healing [Okubo, 1989]. Such a proposal of a new constitutive law with a corresponding microphysical interpretation is a great advance in technology which enables us to implement a complex rate-dependency into earthquake sequence simulations, as well as in understanding of physics of rock friction and earthquake generation process. However, not all experimental data showing complex rate-dependency have been digested and implemented in a rate- and state-dependent framework. In this study, we propose a simple modification to the logarithmic RSF which enables implementation of rate-dependencies ($\partial f/\partial \ln(V)$ and $\partial f_{ss}/\partial \ln(V)$) that change with $\ln(V)$.

Sawai et al. [2014, AGU fall meeting] conducted a series of velocity-step tests with a core sample obtained in JFAST project at 50 MPa effective normal stress σ_e , 50 MPa pore water pressure, various temperatures T from 20 °C to 200 °C, and V from 0.3 to 100 $\mu\text{m/s}$. They found that with increasing V , the rate-dependency $\partial f_{ss}/\partial \ln(V)$ increases from negative to positive at $T = 20$ °C, decreases from positive to negative at $T = 100$ °C and 150 °C, and decreases more remarkably but stays positive in the studied range of V at $T = 200$ °C. In order to account for these complex rate-dependencies, we modified the logarithmic RSF to a quadratic form:

$$f = f_0 + F_1 L_V + F_2 L_V^2 + G_1 L_W + G_2 L_W^2$$

where $L_V = \ln(V/V_0)$ and $L_W = \ln(d_c/V_0\theta)$, f_0 is a reference friction coefficient at a reference slip rate V_0 , F_1 , F_2 , G_1 , and G_2 represent rate-dependencies which are assumed to be given by quadratic functions of ambient temperature T , and θ is the state variable representing recent slowness which evolves with a characteristic slip d_c :

$$d\theta/dt = 1 - V\theta/d_c.$$

Note that at a steady-state, $L_V = L_W$ and

$$f_{ss} = f_0 + (F_1 + G_1)L_V + (F_2 + G_2)L_V^2.$$

This is a generalization of the aging law, the original version corresponding to $F_1 = a$, $F_2 = 0$, $G_1 = -b$, and $G_2 = 0$. We determined the rate-dependency functions by least-squares method from the experimental data by Sawai et al. [2014], and investigated the consequence by means of dynamic earthquake sequence simulations [e.g., Lapusta et al., 2003].

In preliminary simulations, we simulated earthquake sequences on a planer fault in 2-D (mode II) problems with depth-dependent T , depth-dependent σ_e , and a rotation axis to mimic intersection of the fault plane and the surface. Distributions of T and σ_e are determined to be consistent with the heat-flow measurement and modeling by Gao and Wang [2014].

Without additional complexity such as patch-like asperities and high-velocity weakening (e.g., thermal pressurization of pore fluid [Noda and Lapusta, 2013]), earthquakes are nucleated at about 30-50 km downdip from the trench where $\partial f_{ss}/\partial \ln(V)$ is negative regardless of V , and rupture only the shallowest part of the plate interface. The nucleation is preceded by slow slip in the shallower part of the plate interface where $\partial f_{ss}/\partial \ln(V)$ changes its sign with increases V and thus spontaneous acceleration to coseismic slip rate cannot occur. Effect of thermal pressurization and interaction of the system with embedded rate-weakening patches generating earthquakes shall be discussed in the presentation.

Keywords: Earthquake cycle, Friction constitutive law, Numerical simulation, Friction experiment

Relations between wide-area gravity changes and earthquake activity

YAMADA, Kyohei¹ ; MITSUI, Yuta^{2*}

¹Faculty of Science, Shizuoka University, ²Institute of Geosciences, Shizuoka University

We made gravity time series over the world every one month from 2002 to 2014 based on data of the satellite gravity mission GRACE (Gravity Recovery and Climate Experiment). To investigate relations between gravity change and seismic activity, four observation areas (Red Sea, Chile, Tibet and Alaska) were selected. Using seismic activity data of these areas, We counted the earthquake occurrence numbers every one month. A correlative analysis of the gravity changes and the earthquake number of times enabled us to find out that there is a weak correlation between the gravity changes and the earthquake number of times only for the Alaska area. We owed the correlation to some mechanisms of the gravity change leading to the earthquake occurrence in Alaska. Referring to a preceding study about induced earthquakes (Ellsworth, 2013), We investigate two typical mechanisms (fault stress changes due to surface loads by fluid mass increases or reduces in fault friction due to fluid pressure injection). As a result, we consider that the reduction of fault friction by the fluid pressure injection caused the earthquakes, particularly in the northern area of Alaska (>63N) where strike-slip fault mechanisms dominate.

Keywords: Gravity, Seismicity, Induced earthquake, Surface load, Pore fluid pressure

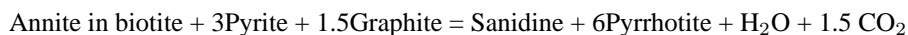
Dynamic fluctuation of redox state during frictional melting and crystallization of graphite-bearing pseudotachylites

NAKAMURA, Yoshihiro^{1*} ; MADHUSOODHAN, Satish-kumar² ; TOYOSHIMA, Tsuyoshi²

¹Graduate School of Science & Technology, Niigata University, ²Department of Geology, Faculty of Science, Niigata University

We carried out a stable carbon isotopic study of graphite-bearing pseudotachylites to characterize the origin, role and behavior of different forms of carbon during frictional melting. The study area, located in the Hidaka Metamorphic belt, exposes metasedimentary rocks and various magmatic intrusions and are extensively deformed as evidenced by the presence of various types of fault rocks such as graphite-bearing cataclasite, ultracataclasite and pseudotachylites. In particular, graphite-bearing pseudotachylites are observed in the brittle shear zones, which are a few mm to maximum 5 cm in width. They are mainly divided into two types (Pst-I and Pst-II) based on the occurrences, microstructures and mineral assemblages of lithic fragments and secondary minerals. The graphite in each domain of Pst-I and Pst-II were separately analyzed for carbon isotopic composition. Disseminated graphite in protolith has a narrow range of $\delta^{13}\text{C}$ values between -23.6 and -25.8 ‰ (n = 13), and cataclasite, ultracataclasite and Pst I also have similar values between -24.1 and -27.0 ‰ (n = 25). On the other hand, the graphite separated from Pst II matrix on slab sections show values between -18.2 and -23.6 ‰ (n = 16), shifting the carbon isotope values to 2-3 ‰ higher from host metamorphic graphite. In particular, there is a clear correlation between stable carbon isotope composition and volume fraction of lithic fragments in each domain.

Our data indicate that metamorphic graphite in fault rocks were converted into $\text{H}_2\text{O}-\text{CO}_2$ or $\text{H}_2\text{O}-\text{CH}_4$ fluids under very-high temperature condition of frictional melting. Subsequently, a part of the COHS fluid re-precipitated as fluid-deposited graphite and the remaining was expelled as COHS fluids into fault zones during quenching stage. On the basis of chemical compositions and mineral assemblages in the pseudotachylites, we attempt to estimate the P-T- $f\text{O}_2$ - $f\text{S}_2$ phase diagram during frictional melting and crystallization of pseudotachylites. The thermal decomposition of biotite coexisting with graphite and sulfide minerals are deduced by following reaction;



The dehydration and decarbonation processes in this reaction are mainly driven by temperature, $f\text{S}_2$, and $f\text{O}_2$, and the breakdown of biotite that is ferromagnesian mineral change the redox state to the more oxidation state at ranges between $\Delta\text{FMQ} +0.5$ to $+3.0$. Such high $f\text{O}_2$ and $f\text{S}_2$ environments are only observed in the domains which show relatively low-temperature condition (Pst I matrix) during frictional melting. On the other hand, in the domains which show high temperature conditions (>1200 degree C) biotite microlite are observed in pseudotachylites instead of pyrrhotite. This suggests the negative jump to biotite stable field of ASM buffer by lowering $f\text{S}_2$ under high-temperature condition. In addition, we tried to estimate the redox state at precipitation stage using graphite-fluid fractionation model. The difference between disseminated graphite and fluid deposited graphite show the positive 2-3 ‰ shifting by carbon isotope fractionation, suggesting the presence of CH_4 -rich COHS fluid during precipitation stage. Under CH_4 - H_2O dominant fluid in COH diagram, we can explain the carbon isotope variation of fluid deposited graphite at around $\Delta\text{FMQ} -3.0$ by hydration reactions during the crystallization of titanite and hydroxyapatite. Such reducing conditions are only observed in the high temperature frictionally melted domains (Pst II matrix).

Thus, oxidation and precipitation processes of graphite are mainly controlled by the breakdown of ferromagnesian minerals and we revealed that the redox state and TOC values dynamically changed within each pseudotachylite matrix. In addition, our data imply that redox state in pseudotachylite sensitively change in melting domains at ranges of $\Delta\text{FMQ} -3.0$ to $+3.0$ as a function of melting temperature and bulk chemistry.

Keywords: Graphite, stable carbon isotope, pseudotachylite, redox state

Thermal and pressure effect on frictional property of smectite: application to the plate boundary earthquakes of Nankai

MIZUTANI, Tomoyo^{1*} ; HIRAUCHI, Ken-ichi¹ ; LIN, Weiren² ; SAWAI, Michiyo³

¹Department of Geosciences, Graduate School of Science, Shizuoka University, ²Kochi Institute for Core Sample Research, Japan Agency for Marine-Earth Science and Technology, ³Department of Earthsciences, Graduate School of Science, Hiroshima University

Along subduction thrust faults, the transformation from smectite to illite at 100-150 °C plays a key role to define the updip limit of the seismogenic zone. If this hypothesis is correct, it is required that smectite exhibits velocity strengthening behavior at in-situ effective normal stress (σ^{eff}) and ~100-150 °C. Here we report results of friction experiments on gouges of pure Na-montmorillonite at σ^{eff} of 10-70 MPa, a pore fluid pressure of 10 MPa, at temperatures of 25-150 °C, and sliding velocities of 0.03-3 $\mu\text{m/s}$, using an oil-medium triaxial testing machine. We found that the coefficient of friction (μ) ranges from 0.056 to 0.120. At temperatures of 20 to 60 °C, μ systematically decreased with increasing σ^{eff} , while at 90-120 °C, it increased with increasing σ^{eff} . With increasing σ^{eff} , the velocity dependence of friction ($a-b$) became negative at 25-90 °C and positive at 120 °C. Therefore, we suggest that smectite friction promotes stable slip along the decollement at the shallow Nankai subduction zone.

Keywords: subduction thrust fault, decollement, aseismogenic zone, smectite, laboratory experiment, velocity dependence of friction

Dependences of pore pressure on elastic wave velocities and Vp/Vs ratio for thermally cracked gabbro

NISHIMURA, Kaya^{1*}; UEHARA, Shin-ichi¹; MIZOGUCHI, Kazuo²

¹Graduate School of Science, Toho University, ²Central Research of Electric Power Industry

Marine seismic refraction have found that there are high Vp/Vs ratio regions in oceanic crusts at subducting oceanic plates. For example, Cascadia subduction zone (2.0~2.8) (Audet *et al.*, 2009), Nankai Trough subduction zone (≥ 2.03) (Kodaira *et al.*, 2004), Chile subduction zone (>1.8) (Marcos *et al.*, 2012). Christensen (1984) conducted laboratory measurements of compressional and shear wave velocities (Vp and Vs, respectively) of basalt and dolerite, which are ones of major rocks in oceanic crust, and the results of Vp/Vs ratio were high enough to explain the observation for basalt, while for the measurements of dolerite, the results of the Vp/Vs ratio were not high enough. This difference may reflect the difference on porosity; porosities of the basalt and dolerite specimens were approximately 4% and 1%, respectively. Peacock *et al.* (2011) also indicated that Vp/Vs ratio is high when porosity and pore pressure is high. But relationships between of fracture distribution and Vp and Vs for gabbro have not investigated in detail. This study reports the results of measurements of Vp and Vs at controlled confining and pore pressure and estimation of Vp/Vs ratio for thermally cracked gabbro, which is one of major rocks in oceanic crust and can mainly distribute in the high Vp/Vs ratio zone.

To prepare specimens with various fracture distribution, the rock specimens were heated at 500 °C and 700 °C for 24 hours. We also did measurement with an intact rock specimen. We measured Vp and Vs by using transmission method, with putting piezoelectric elements on the specimen. Before measuring Vp and Vs at confining and pore pressure, we did measurements under atmospheric pressure, and revealed the anisotropy of the velocities of up to 10 %. We measured Vp and Vs for four directions at confining and pore pressure. Confining pressure was constant, 50 MPa, and pore pressure was decreased from 49 to 0.1 MPa and then increased to 49 MPa. For the specimen thermally cracked under 500 °C, when pore pressure was 49 MPa, Vp/Vs ratio was 2.0~2.1. This is close to the value of Vp/Vs which was obtained by marine seismic refraction. On the other hand, the Vp/Vs ratio of intact rock did not change as pore pressure changed and were almost constant, approximately 1.5.

At the presentation, we will also show the results of measurements of fracture distribution such as fracture densities or apertures, and reveal the relationship between them and the results of the experiment.

This work was supported by JSPS KAKENHI Grant Number 26400492.

Keywords: Gabbro, Vp/Vs ratio, Elastic wave velocity, High pore pressure